DYRK3 Dual-specificity Kinase Attenuates Erythropoiesis during Anemia[*]

Olga Bogacheva[‡], Oleg Bogachev[‡], Madhu Menon[‡], Arvind Dev[‡], Estelle Houde[‡], Elizabeth I. Valoret[§],
Haydn M. Prosser[¶], Caretha L. Creasy[§], Susan J. Pickering[¶], Evelyn Grau[¶], Kim Rance[¶], George P. Livi[§], Vinit Karur[‡],
Connie L. Erickson-Miller[§], and Don M. Wojchowski[‡1]

From the ‡Stem and Progenitor Cell Biology Program, Molecular Medicine Division, Maine Medical Center Research Institute,
Scarborough, Maine 04074, §GlaxoSmithKline, Collegeville, Pennsylvania 19426, and ¶GlaxoSmithKline,
CM195AW Harlow, United Kingdom

During anemia erythropoiesis is bolstered by several factors including KIT ligand, oncostatin-M, glucocorticoids, and erythropoietin. Less is understood concerning factors that limit this process. Experiments performed using dual-specificity tyrosine-regulated kinase-3 (DYRK3) knock-out and transgenic mice reveal that erythropoiesis is attenuated selectively during anemia. DYRK3 is restricted to erythroid progenitor cells and testes. DYRK3$^{-/-}$ mice exhibited essentially normal hematological profiles at steady state and reproduced normally. In response to hemolytic anemia, however, reticulocyte production increased severalfold due to DYRK3 deficiency. During 5-fluorouracil-induced anemia, both reticulocyte and red cell formation in DYRK3$^{-/-}$ mice were elevated. In short term transplant experiments, DYRK3$^{-/-}$ progenitors also supported enhanced erythroblast formation, and erythropoietic advantages due to DYRK3-deficiency also were observed in 5-fluorouracil- treated mice expressing a compromised erythropoietin receptor EPOR-HM allele. As analyzed ex vivo, DYRK3$^{-/-}$ erythroblasts exhibited enhanced CD71^{pos}Ter119^{pos} cell formation and ^{3}HdT incorporation. Transgenic pA2gata1-DYRK3 mice, in contrast, produced fewer reticulocytes during hemolytic anemia, and pA2gata1-DYRK3 progenitors were compromised in late pro-erythroblast formation ex vivo. Finally, as studied in erythroid K562 cells, DYRK3 proved to effectively inhibit NFAT (nuclear factor of activated T cells) transcriptional response pathways and to co-immunoprecipitate with NFATc3. Findings indicate that DYRK3 attenuates (and possibly apportions) red cell production selectively during anemia.

Erythroid cell production is highly regulated, and ~10^{11} red blood cells are formed daily by the adult erythron. During anemia, erythropoiesis can be accelerated further by several factors. Examples include reinforcing signals provided via KIT

ligand (1), bone morphogenetic protein 4 (2), oncostatin-M (3), glucocorticoids (4), and erythropoietin (EPO)[2] receptor signals (5). Certain factors that set limits on such stress erythropoiesis also have been described. As tumor necrosis factor α (TNFα) orthologues, TRAIL (TNF-related apoptosis-inducing ligand) and Fas ligand each can attenuate erythroid progenitor cell proliferation and/or survival (6, 7). Negative feedback components integral to KIT and EPO receptor signaling circuits also are operative. These include SHP1 and PTP1B phosphatases (8, 9), CIS, SOCS3, and SPRED1 as attenuators of JAK2 (Janus protein tyrosine kinase 2) and KIT kinases (5, 10, 11), and additional adaptor proteins within select signal transduction pathways (e.g. LNK and SH2B1) (12, 13). Previously, our laboratories reported on the erythroid-restricted expression of a novel DYRK (dual-specificity tyrosine-regulated kinase) family dual-specificity kinase, DYRK3/REDK (14, 15). Upon antisense oligonucleotide inhibition of DYRK3 expression, enhanced murine and human colony-forming unit-erythroid formation also was observed (14, 15). Interestingly, this suggested that DYRK3 might act to attenuate erythroblast development.

DYRK kinase orthologues also exist in lower species and have been studied functionally in yeast, Dictyostelium, Caenorhabditis elegans, and Drosophila. In Saccharomyces cerevisiae, stress in the form of glucose depletion stimulates the DYRK kinase YAK1p. YAK1p then phosphorylates a Pop2p transcription factor complex which regulates cell cycle entry and progression (16). In Dictyostelium, a YAKA orthologue likewise is stimulated due to nutrient depletion and acts to inhibit growth stage genes in part by phosphorylating and inhibiting a cprD growth-phase factor (17). YAKA loss-of-function also leads to accelerated cell growth. In C. elegans, a minibrain kinase DYRK kinase exerts inhibitory effects, but these are directed toward a MEI-1 substrate which itself attenuates the transition of oocytes to developing zygotes (18). Finally, in Drosophila, a "minibrain" phenotype (Mnb) has been attributed to the mutation of minibrain as a DYRK family kinase (19). Minibrain is important for optic and central lobe development and best corresponds to DYRK1a among five vertebrate DYRKs (20, 21).

Vertebrate DYRKs are best studied in man and mice, with two classes represented. Class-1 includes DYRK1a and

---

[1] To whom correspondence should be addressed: Stem and Progenitor Cell Biology Program, Maine Medical Center Research Institute, 81 Research Dr., Scarborough, ME 04074. Fax: 207-885-8179; E-mail: wojchd@mmc.org.

[2] The abbreviations used are: EPO, erythropoietin; BFUe, burst-forming unit-erythroid; DYRK, dual-specificity tyrosine-regulated kinase; SCF, stem cell factor; ^{3}HdT, tritiated deoxythymidine; FALS, forward-angle light scatter; GFP, green fluorescent protein; FACS, fluorescence-activated cell sorter.

DYRK1b/M1RK kinases. DYRK1a interestingly maps to a critical region of Down syndrome trisomy-21 (22). Moreover, mice haplo-insufficient for DYRK1a exhibit decreased brain size and compromised pyramidal cell complexity (23, 24), and transgenic expression of a human BAC DYRK1a affects hippocampal synaptic plasticity (25). DYRK1a also has been demonstrated to phosphorylate the neuronal proteins α-synuclein (26) and synaptojanin-1 (27) (but unlike DYRKs 2–4, encodes a consensus nuclear localization signals and is predominantly nuclear) (20, 21). DYRK1b is structurally most related to DYRK1a. To date, gene disruption experiments have not revealed specific roles for DYRK1b. However, DYRK1b has been implicated as an anti-apoptotic factor within several solid tissue tumors (28, 29) and is expressed in pancreatic adenocarcinomas at elevated levels (and may act downstream of K-Ras) (30).

Among class 2 DYRKs, DYRK4 expression is predominant in testes, yet is apparently nonessential (31). DYRK2 is more broadly expressed and, like at least certain DYRKs of lower species, appears to be stress-activated and to attenuate cell growth (16, 17). In recent investigations by Taira *et al.* (32), this is revealed to involve DYRK2 phosphorylation of p53 at Ser-46 and the stimulation of pro-apoptotic actions via p53-AIP. In its gene and kinase domain substructures, DYRK3 is most related to DYRK2 (33), is predominantly cytoplasmic, and among hematopoietic cells is narrowly restricted in its expression to erythroid lineage (14, 15). Similar to YAKA (17) and YAK1p (34), DYRK3 also has been associated with cAMP-dependent protein kinase (PKA) as well as cyclic AMP response element-binding protein (CREB) pathways (35). DYRK3 *in vivo* functions, however, are poorly understood.

To test hypothesized roles of DYRK3 as a candidate lineage-specific regulator of erythropoiesis, we presently have generated $DYRK3^{-/-}$ mice and have examined effects of DYRK3-deficiency on erythropoietic capacities. In several anemia models, and in analyses of primary bone marrow erythroblast development *ex vivo*, the absence of DYRK3 conferred a meaningful advantage for erythroid cell formation. By comparison, transgenic expression of DYRK3 from a pA2gata1 vector (36, 37) significantly attenuated late-stage erythropoiesis. We, therefore, propose that DYRK3 may act via intrinsic erythroid cell mechanisms to selectively place an upper limit on stress erythropoiesis. One such mechanism for DYRK3 action which was tested involved possible modulation of NFAT activity. This was based on recently discovered intersections between DYRKs and NFAT signaling as investigated via small interfering RNA studies in *Drosophila* S2 cells (38). In human erythroid cells, DYRK3 in fact is presently shown to efficiently inhibit NFAT transcriptional activation capacities. Based on these characterized suppressor properties, DYRK3 may further constitute a new rational target for small molecule inhibitors aimed at treating acute anemia. Potential significance is underlined by an emerging need for alternatives to EPO for the treatment of anemia due to cancer and chemotherapy (39).

EXPERIMENTAL PROCEDURES

Mouse Models—m*DYRK3* genomic clones were isolated from a 129svJ λ phage library by hybridization to an h*DYRK3* cDNA. *DYRK3* gene deletion was in E14 ES cells using a floxed PGKneo targeting vector. Targeted cells were injected into C57BL/6J blastocysts. Progeny of chimerics were bred with C57BL/6 mice (five generations) and with C57BL/6 EII2A-Cre mice. $DYRK3^{+/-}$ mice were bred to yield $DYRK3^{-/-}$ mice (which were further backcrossed to C57BL/6 mice). Wild-type controls were $DYRK3^{+/+}$ littermates or C57BL/6J stocks. EpoR-HM mice (expressing a minimal EPO receptor allele) were as described (40). PCR primer pairs were as follows: wild type *DYRK3* allele, 5'-CCA-GCT-GCT-TCG-AGT-ATC-AGA-AG-3' and 5'-GTA-CTT-GGC-ACG-TTT-GGA-TTG-C-3'; $DYRK3^{-/-}$ allele, 5'-GAG-GAG-ATC-CGG-ATC-TTG-GAG-CAT-CTT-3' and 5'-GTA-AGT-CCC-TCC-CCG-CTC-TGA-GGG-3'. Transgenic pA2gata1-DYRK3 mice were prepared using an Myc epitope-tagged mDYRK3 cDNA (15) within a pA2gata1 vector (36, 37). For BDF1 pronuclei injections (15, 36) a 5'-KpnI → 3'-SalI fragment was used. For all mice and protocols used (see below), review and approval was provided by Institutional Animal Care and Use Committees.

Hematological Analyses—Blood cell counts were analyzed with an Advia system (Bayer). Hematocrits also were assayed by microcapillary centrifugation. Blood smears were stained with new methylene blue, and reticulocytes were assayed using Retic-COUNT (BD Biosciences). Burst- and colony-forming unit-erythroids were assayed in MethoCult M3234 medium (Stem Cell Technologies) containing murine SCF (100 ng/ml) plus EPO (5 units/ml). Colony forming unit granulocytic/monocytic colonies were assayed in MethoCult GF M3534 containing murine SCF (50 ng/ml), murine interleukin-3 (IL-3; 10 ng/ml), and human IL-6 (10 ng/ml).

Anemia Models—Hemolytic anemia was induced by phenylhydrazine (60 mg/kg, 1 and 24 h). 5-Fluorouracil-induced anemia was generated via intraperitoneal injection (150 mg/kg). In transplantations, B6.Ptprca.GPI-a recipients were irradiated (550 rads) at 5 and 1.5 h before transplant. Donor bone marrow from $DYRK3^{-/-}$ or C57BL/6 controls was injected via tail vein (5×10^6 cells). At day 13, recipients were analyzed for donor contributions based on Ly5.2 positivity, and frequencies of splenic CD71^{high}Ter119^{pos} erythroblasts were determined (together with Ly5.2^{pos} B220^{pos} progenitors).

Erythroblast Expansion and Proliferation Assays—Progenitor cells from $DYRK3^{-/-}$ and wild-type bone marrow were prepared as detailed previously (3, 40). Erythroid progenitors were expanded in SP34 medium (Invitrogen) supplemented with 2.5 units/ml EPO, 100 ng/ml murine SCF (Peprotech Inc.), 1 μM dexamethasone, 1 μM β-estradiol, 75 μg/ml human transferrin, 1% bovine serum albumin (Stem Cell Technologies), and 0.1 mM 2-mercaptoethanol (SP34-EX medium). At 24 h, 0.6 volumes of SP34-EX were added. At 48 h, cells were replated. In [3]HdT incorporation assays, Kit^{pos}CD71^{high} progenitors were isolated (by lineage depletion and magnetic cell sorting and separation system) and plated in SP34-EX medium (1×10^5 cells/ml) with erythropoietin and/or SCF. At 20 h, 1 μCi of [3]HdT was added, and at 5 h, incorporation rates were determined.

Flow Cytometry—In flow cytometry (BD FACScalibur), washed cells (1×10^6 per 0.2 ml phosphate-buffered saline, 0.1% bovine serum albumin) were incubated with rat IgG (1 μg)

and stained with 1 μg each of APC-Ly5.2 or Ly5.1 (eBioscience), fluorescein isothiocyanate (FITC)-B220, or PE-Ter119 plus FITC-CD71 (BD Biosciences) antibodies. Analyses of erythroblast development *ex vivo* utilized PE-Ter119 plus FITC-CD71.

Reverse Transcription and Quantitative PCR—RNA was prepared using TRIzol reagent (Invitrogen). cDNA was prepared with SuperScript III (Invitrogen). Quantitative PCR utilized iQ SYBR® Green and an i-Cycler (Bio-Rad). PCR primer pairs were from SuperArray Bioscience as follows: Nfatc1, NM_016791; Nfatc2, NM_010899; Nfatc3, NM_010901; Nfatc4, NM_023699; Nfat5, NM_018823; Dyrk3, NM_145508; β-actin, NM_007393.

Cell Lines and Transcriptional Reporter Assays—K567/NFAT-Luc cells (Panomics) were maintained as recommended (in the presence of 100 μg/ml hygromycin-B). Lines expressing (Myc)DYRK3 or GFP only (vector control) were prepared by transduction with VSVg-packaged MIEG3 retroviruses. Stably transduced GFP^{pos} populations were isolated by FACS (BD Biosciences FACS Aria). Endogenous NFAT was activated using A23187 plus phorbol 12-myristate 13-acetate. Induced luciferase levels were assayed using Promega reagents (#E4030 system) and a Turner Modulus luminometer.

Western Blotting and Immunoprecipitations—Lysates from transfected 293 cells or primary erythroblasts were prepared as described previously (41). In immunoprecipitations, rabbit antiserum to a DYRK3 peptide was utilized. Western blots utilized antibodies to a Myc epitope (Sigma) or to NFATc3 (Cell Signaling).

RESULTS

DYRK3 Deficiency Confers Erythropoietic Advantages during Anemia due to Hemolysis, 5-Fluorouracil, or Marrow Transplantation—To advance loss-of-function analyses, gene targeting was used to disrupt exon-3 of the *DYRK3* gene, which encodes the DYRK3 catalytic domain and unique C-terminal region (33). Exon-3 targeting in ES cells and derived mice was confirmed initially by Southern blotting and subsequently by genomic PCR (Fig. 1). Reverse transcription-PCR further was employed to assess transcript expression in primary erythroblasts expanded from the bone marrow of $DYRK3^{-/-}$ mice. In initial analyses of phenotypes in $DYRK3^{-/-}$ mice, no effects of DYRK3 deficiency on reproductive capacities or other basic physiological parameters were observed (despite high level expression in testes) (14, 15). With regard to hematopoiesis, peripheral blood cell counts and frequencies of myeloid progenitor cells in marrow (as determined via colony-forming assays) were essentially unaffected (data not shown). Within spleen and among $DYRK3^{-/-}$ mice, however, BFUe levels were reproducibly decreased. Specifically, $DYRK3^{-/-}$ BFUe frequencies were 37.3 ± 1.5 per 2 × 10^5 splenocytes *versus* 69.3 ± 4.6 per 2 × 10^5 splenocytes for wild-type congenic controls. For splenic granulocytic and monocytic lineages, no significant differences between $DYRK3^{-/-}$ progenitors and $DYRK3^{+/+}$ progenitors were observed (data not shown). When the erythron is stressed, increases in splenic erythroid progenitor cell levels often are observed (5, 42). Observed decreases in splenic BFUe in $DYRK3^{-/-}$ mice, therefore, were consistent with possibly
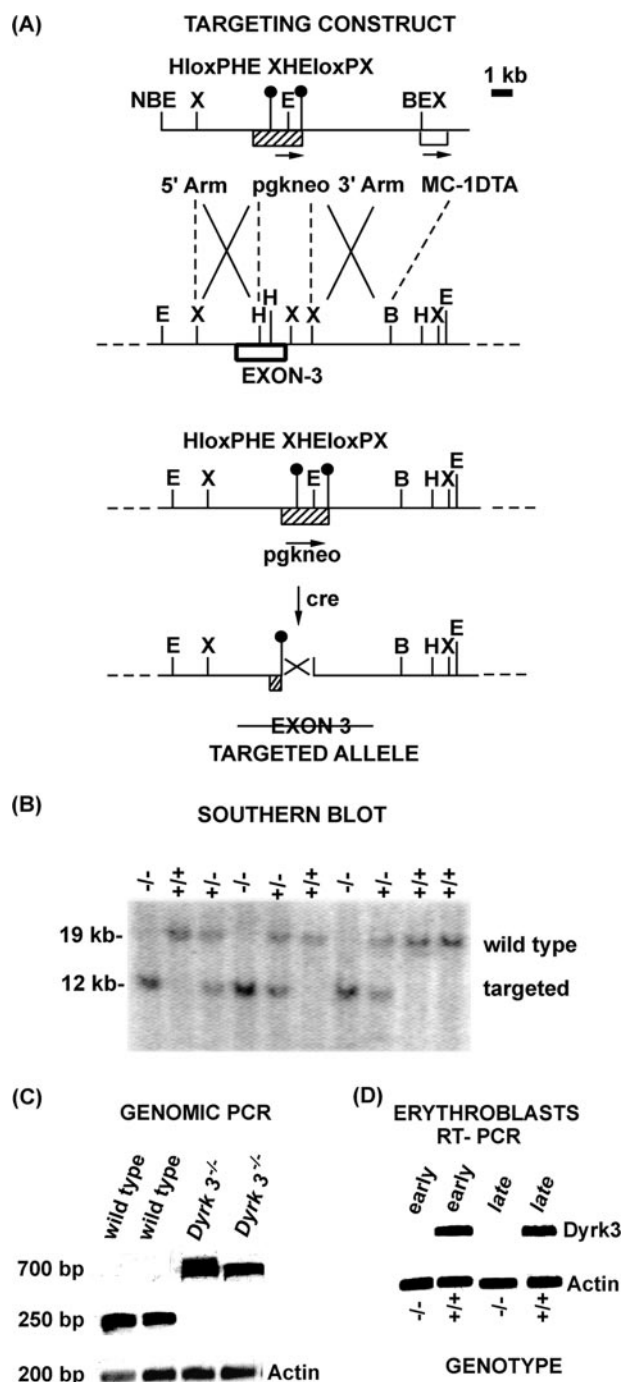

FIGURE 1. **Disruption of the murine *DYRK3* gene.** *A*, *DYRK3* gene-targeting strategy. Targeting was with a floxed pgk-Neo cassette, which was then deleted from ES cells before blastocyst fusion. The targeted DYRK3-null allele retains a 5′-portion of exon-3 and two small upstream exons but lacks the 222 codons of exon-3 plus ~2 kilobases (*kb*) of 3′-untranslated sequence (*B*, BamHI; *E*, EcoRII; *H*, HindIII; *N*, NotI; *X*, XbaI). *B*, in Southern blot analyses of *DYRK3* loci, genomic DNA was digested with EcoRV and hybridized with domains external to the targeting vector. *C*, PCR-based *DYRK3* genotyping and reverse transcription (*RT*)-PCR of *DYRK3* transcripts in bone marrow erythroblasts after expansion in SP34-EX medium. *D*, early erythroblasts correspond to a Kit^{pos}CD71^{high} stage; late erythroblasts correspond to a CD71^{high}Ter119^{pos} stage. MC-1DTA, diptheria toxin A cassette.

advantaged erythropoiesis. This notion was next tested in several anemia models.

Mice first were treated with phenylhydrazine to induce hemolytic anemia. At days 8 and 12, $DYRK3^{-/-}$ mice produced
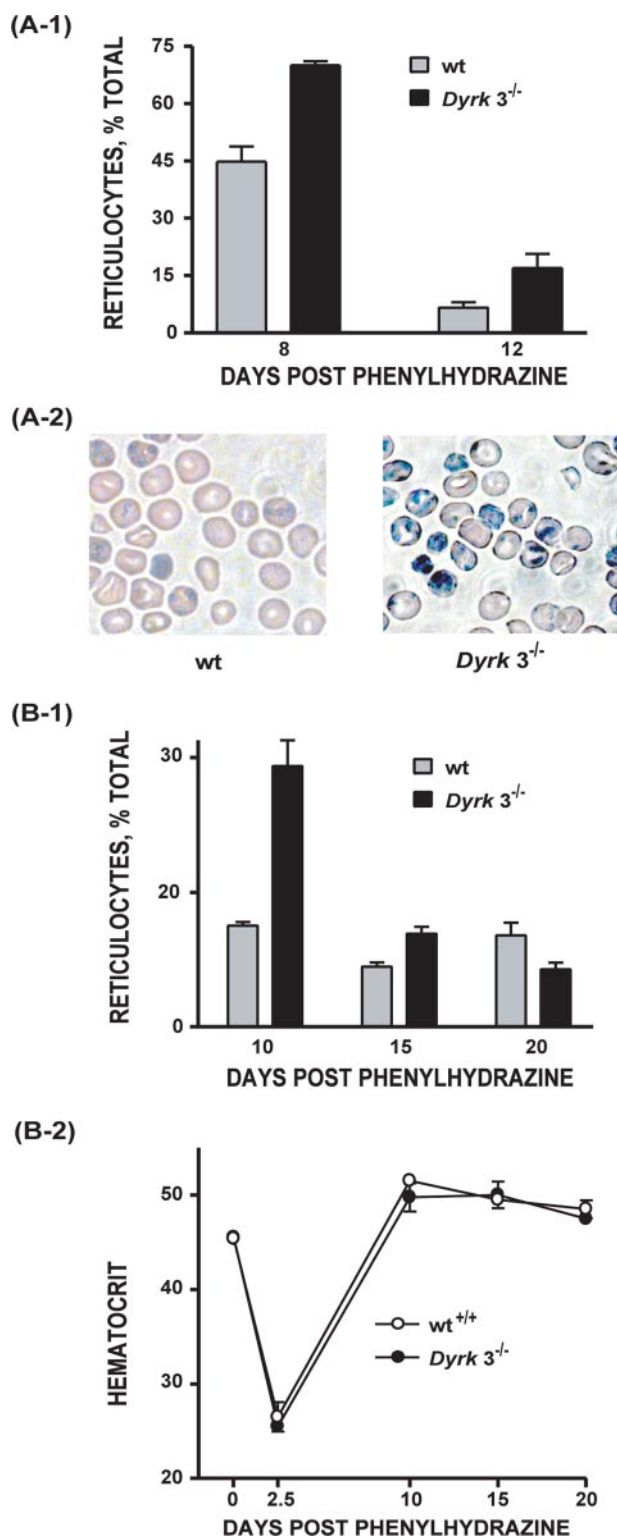
(A-1)

(A-2)

wt   *Dyrk 3*[−/−]

(B-1)

(B-2)

FIGURE 2. **Increased reticulocyte production in *DYRK3*^{−/−} mice during phenylhydrazine-induced hemolytic anemia.** *A, DYRK3*^{−/−} and wild-type (*wt*) mice were dosed with phenylhydrazine at 1 and 24 h (60 mg/kg, *n* = 4 mice per group). On days 8 and 12 reticulocyte levels were determined (means ± S.D.) *A1*, reticulocyte populations also were analyzed by methylene blue staining (*A2*). *B*, in independent experiments reticulocyte production was monitored over an extended time-course (*B1*). Hematocrits in phenylhydrazine-treated *DYRK3*^{−/−}, and wild-type congenic controls also were determined (*B2*).
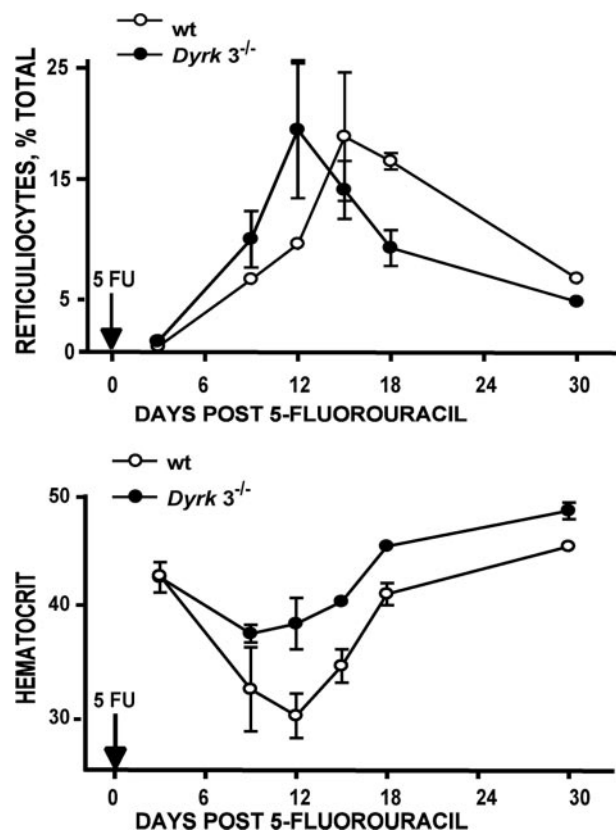

FIGURE 3. **Increased reticulocyte production in *DYRK3*^{−/−} mice during 5-fluorouracil induced anemia.** *DYRK3*^{−/−} and wild-type (*wt*) control mice were administered 5-fluorouracil (150 mg/kg, *n* = 3 mice per group). At the indicated intervals, reticulocyte levels and hematocrits were determined. For *DYRK3*^{−/−} mice, note the elevated production of reticulocytes and red cells.

reticulocytes at levels 1.6- and 2.4-fold above wild-type controls, respectively (Fig. 2*A*). In repeated experiments this advantage was maximal at day 10 post-phenylhydrazine dosing (Fig. 2*B*) but was not reflected by substantially increased hematocrits. For DYRK3-deficient red cells, this was not associated with any detectable increase in erythrocyte sensitivity to lysis by phenylhydrazine or hyposmotic solutions. Next, *DYRK3*^{−/−} and congenic control mice were treated with 5-fluorouracil to deplete proliferating early progenitor cell pools. In this distinct anemia model, reticulocyte production in *DYRK3*^{−/−} mice again was significantly elevated over controls (Fig. 3, *upper panel*). DYRK3 deficiency furthermore proved to protect against the sharp drop in hematocrits experienced by wild-type controls after 5-fluorouracil dosing (Fig. 3, *lower panel*). Capacities of donor *DYRK3*^{−/−} progenitor cells to contribute to short term reconstitution in irradiated recipients also were assessed. Here, donor contributions were determined based on CD45-5.1 marking of hosts, and mice with >90% CD45-5.2 donor contributions were considered. Analyses were of donor-derived CD71^{high}Ter119^{pos} erythroblasts in spleen at day-13 post-transplantation. Representative outcomes are illustrated in Fig. 4 and reveal an approximate 2-fold increase in *DYRK3*^{−/−} CD71^{high}Ter119^{pos} erythroblast formation. By direct comparison, no such difference was observed between *DYRK3*^{−/−} and control donor-derived lymphoid B220^{pos} cells.
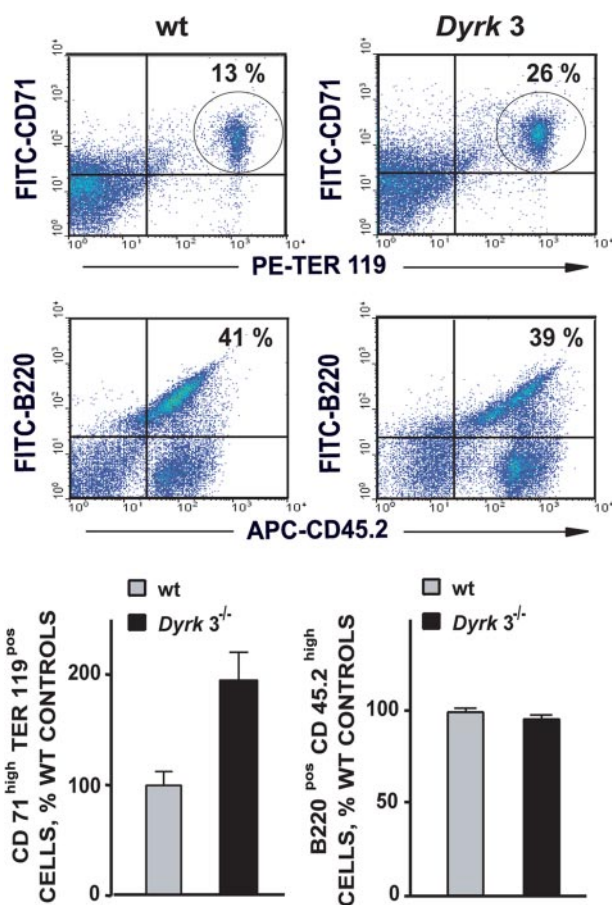
FIGURE 4. **Contributions of DYRK3-deficient progenitors to the erythroid lineage are enhanced during short term repopulation.** In transplantation experiments, bone marrow preparations from donor *DYRK3*$^{-/-}$ or wild-type (*wt*) control mice were used to repopulate irradiated Ly5.1-marked recipients. On day 13 and for mice with >90% Ly5.2 engraftment, levels of splenic CD71^{high} Ter119^{pos} erythroblasts were determined (in parallel with Ly5.2^{pos} B220^{pos} B-cells). Also graphed are mean frequencies (±S.D.) of repopulating *DYRK3*$^{-/-}$ and control CD71^{pos}Ter119^{pos} cells among *n* = 3 such recipients.

DYRK3$^{-/-}$ *Erythroblasts Develop at Accelerated Rates ex Vivo*—To better assess predicted erythroid cell intrinsic effects of DYRK3, a primary culture system was implemented to analyze the stepwise development of bone marrow-derived DYRK3$^{-/-}$ erythroblasts *ex vivo*. This involved the expansion of bone marrow progenitors in a serum-free SP34-EX medium with optimized supplements and sources (including KIT ligand, EPO, transferrin, bovine serum albumin, dexamethasone and β-estradiol). Erythroblast expansion depended upon KIT ligand and dexamethasone (as well as EPO), and in these regards reflects stress erythropoiesis (1, 3, 4). At day 2.5 of culture, control erythroblasts reproducibly developed from Kit^{high}CD71^{low}Ter119^{neg} progenitors toward CD71^{high} Ter119^{low} erythroblasts (Fig. 5*A*, *left panels*). CD71 corresponds to the transferrin receptor, and Ter119 is a late erythroid-specific marker (43, 44). On day 3.5, cells developed further at significant frequencies to a Kit^{neg}CD71^{high}Ter119^{high} stage. By direct comparison, *DYRK3*$^{-/-}$ erythroblasts developed similarly but advanced at increased frequencies (within the same timeframe) to a CD71^{high}Ter119^{high} stage (Fig. 5*A*, *right panels*). This advanced rate of *DYRK3*$^{-/-}$ erythroblast development was reproducible both within and among experi-

ments (Fig. 5*B*). In addition, differences in hemoglobinization levels between *DYRK3*$^{-/-}$ and control erythroblasts often were visibly obvious (Fig. 5*C*). Finally, rates of EPO-dependent ^{3}HdT incorporation also were assayed using isolated Kit^{pos}CD71^{high} wild-type and *DYRK3*$^{-/-}$ progenitors. *DYRK3*$^{-/-}$ erythroblasts consistently exhibited increased responses (Fig. 5*D*).

DYRK3 Deficiency Enhances Stress Erythropoiesis in 5-Fluorouracil-treated EpoR-HM Mice—The above analyses suggest that DYRK3 suppresses erythropoiesis at least in part during an EPO-dependent developmental phase. *In vivo* effects of EPO, therefore, were assessed in *DYRK3*$^{-/-}$ mice and congenic wild-type controls. Specifically, *DYRK3*$^{-/-}$ and wild-type mice were dosed with Darbepoietin, and reticulocyte and red cell production then were assayed through time. As outlined in Table 1 and as assayed at day-8, *DYRK3*$^{-/-}$ mice exhibited modest yet significant increases in reticulocyte levels over controls. In *DYRK3*$^{-/-}$ mice, a trend toward enhanced hematocrit levels also was observed but fell short of clear statistical significance.

DYRK3$^{-/-}$ mice further were bred onto an *EpoR-HM* line which exhibits defective stress erythropoiesis. Specifically, *EpoR-HM* is a knocked-in phosphotyrosine-null EPO receptor allele that supports steady-state erythropoiesis but falters in its ability to support erythropoiesis during 5-fluorouracil- or phenylhydrazine-induced anemia (3). *EpoR-HM:DYRK3*$^{-/-}$ mice and *EpoR-HM* controls were treated with 5-fluorouracil. Reticulocyte and red cell production were then assayed over a 25-day period. At days 10–20, the absence of DYRK3 in *EpoR-HM:DYRK3*$^{-/-}$ mice resulted in a significant attenuation of the severe anemia otherwise incurred by *EpoR-HM* mice (Fig. 6). In particular, hematocrits in *EpoR-HM:DYRK3*$^{-/-}$ mice were maintained at greater than 22.5% but as shown here (and in recent studies by Menon *et al.* (3)) fell more sharply in *EpoR-HM* mice. In *EpoR-HM* mice, reticulocyte levels remained elevated at days 12–20 (as compared with *EpoRH:DYRK3*$^{-/-}$ mice) presumably due to sustained signals for recovery from sharp anemia.

Transgenic Expression of DYRK3 Attenuates Erythropoiesis—In complementing experiments, effects of enforcing DYRK3 expression within erythroid progenitor cells were assessed. In particular, a Myc epitope-tagged *mDYRK3* cDNA was cloned to pA2gata1 (15, 36, 37), and an excised KpuI → SalI cassette was used to prepare transgenic pA2gata1-DYRK3 mice (Fig. 7, *A*, *1* and *2*). In two selected lines, expression at the protein level in primary bone marrow erythroblasts also was assessed and demonstrated by Western blotting (with an anti-Myc antibody, data not shown). In these mice, as in DYRK3-null mice, no substantial effects of perturbed DYRK3 expression on steady-state erythropoiesis were observed. During phenylhydrazine-induced anemia, however, reticulocyte levels were significantly attenuated (Fig. 7*B*). In further *ex vivo* analyses of erythroid sphenocytes from phenylhydrazine-treated mice, three additionally interesting effects of pA2gata-enforced DYRK3 expression on erythropoiesis were observed. First, levels of Ter119^{pos} erythroid progenitor cells in spleens from pA2gata1-DYRK3 mice were significantly decreased (*i.e.* from ~75% in BDF1 littermates to ~55% among pA2gata1-DYRK3 transgenics) (Fig. 7*C*). Second, when these splenic pro-erythroblasts were cultured short term and assessed for sub-stages of development
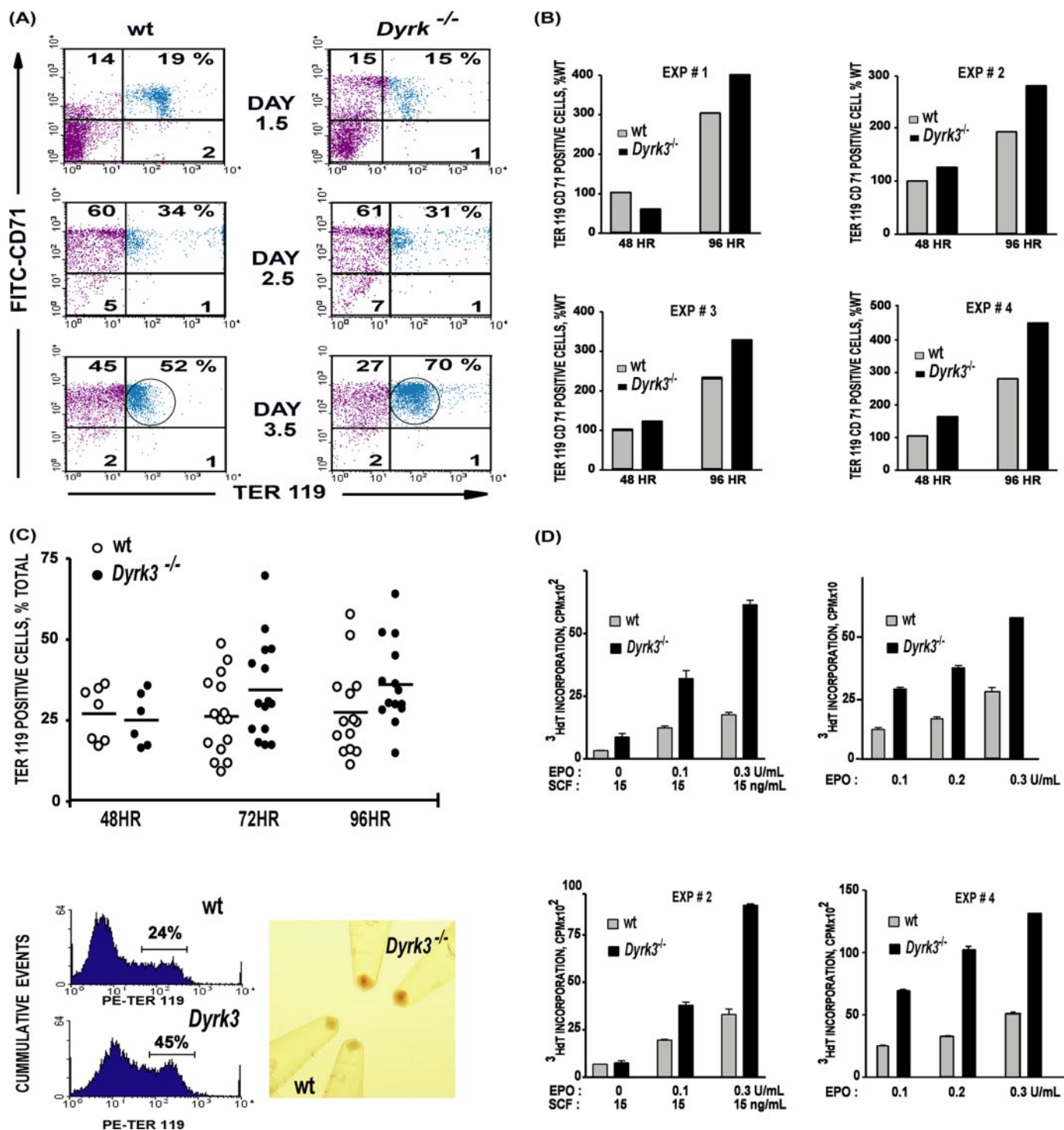
FIGURE 5. **Accelerated development of *DYRK3*$^{-/-}$ erythroblasts *ex vivo*.** *A*, a system was implemented in which bone marrow erythroid progenitor cells develop from CD71^{low}Ter119^{neg} (pro.)erythroblasts (day 1.5) to CD71^{high}Ter119^{neg} erythroblasts (day 2.5) and further to CD71^{high}Ter119^{pos} erythroblasts (day 3.5). In this system *DYRK3*$^{-/-}$ progenitors were observed to progress at increased frequencies to CD71^{high}Ter119^{pos} erythroblasts (*circled populations*). *wt*, wild type. *B*, this above-outlined developmental advantage was observed in repeated experiments, each including pairs of *DYRK3*$^{-/-}$ and control mice (mean frequencies of CD71^{pos}Ter119^{pos} cells are graphed). *C*, increased Ter119^{pos} erythroblast formation among *DYRK3*$^{-/-}$ mice. Marrow-derived progenitor cells from wild-type and *DYRK3*$^{-/-}$ mice were cultured in SP34-EX medium. At 48, 72, and 96 h, frequencies of Ter119^{pos} erythroblasts were determined. Each symbol represents frequencies of Ter119^{pos} erythroblasts formed in preparations from independent mice. *Horizontal bars* index over all mean values among groups (*upper panel*). A representative profile for Ter119 cell surface marker staining also is shown, and visibly detectable increases in hemoglobinization among *DYRK3*$^{-/-}$ erythroblasts (microcentrifuged cells at 96 h) also are illustrated (*lower panel*). *D*, SCF- and Epo-dependent ^{3}HdT incorporation is increased in *DYRK3*$^{-/-}$ erythroblasts. Kit^{pos}CD71^{high} erythroblasts were isolated from expansion cultures, cultured for 20 h in the presence of SCF and/or EPO, and pulsed with ^{3}HdT. Outcomes of four independent experiments are graphed (means ± S.E.).

TABLE 1

DYRK 3 deficiency enhances Darbepoietin-stimulated reticulocyte and red cell formation

	Reticulocytes		Hematocrit	
	Day 8[a]	Day 16[a]	Day 8[a]	Day 16[a]
$DYRK3^{-/-}$	20.9 ± 0.2[b]	2.4 ± 0.2	61.3 ± 1.1	48.5 ± 1.0
Wild type	13.9 ± 2.3	2.4 ± 0.9	56.3 ± 3.9	52.0 ± 1.7

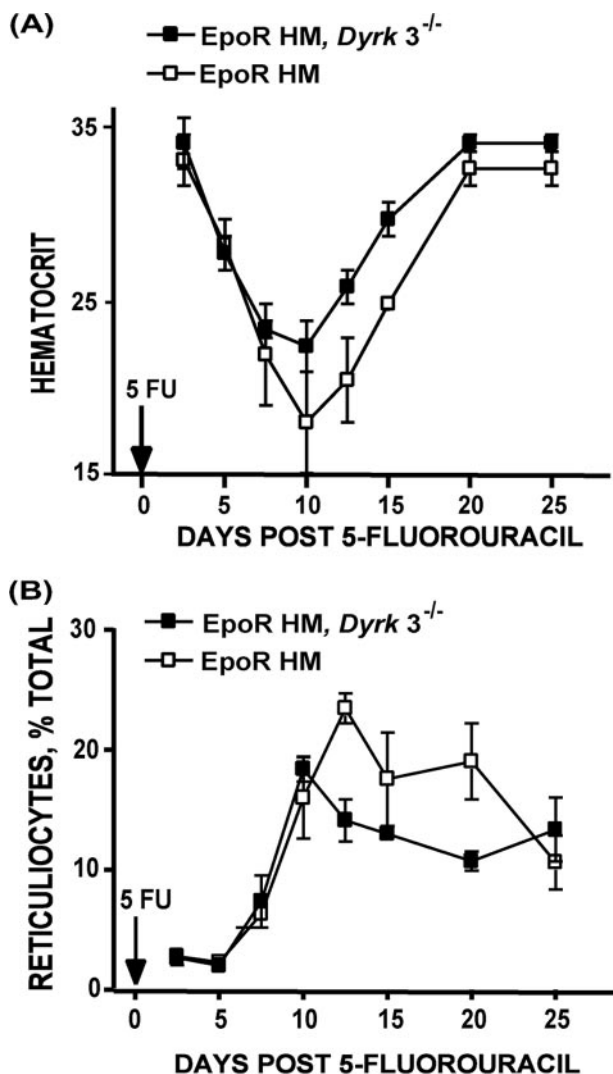[a] Days post-Darbepoietin injection.
[b] $p < 0.05$.

FIGURE 6. **$DYRK3^{-/-}$ deficiency enhances erythropoiesis during 5-fluorouracil-induced anemia in EpoR-HM mice.** Mice expressing the knocked-in minimal EPO receptor allele EpoR-HM were crossed with $DYRK3^{-/-}$ mice to yield compound $EpoR$-HM:$DYRK3^{-/-}$ mice. In these mice and in EpoR-HM controls, anemia was induced with 5-fluorouracil (150 mg/kg). At the indicated time points, hematocrits (*panel A*) and reticulocyte levels (*panel B*) were determined (means $\pm$ S.E., $n = 4$).

(based on CD71 levels) an obvious difference was exhibited. Specifically, Ter119^{pos} progenitors from pAgata1-DYRK3 mice were attenuated in development and accumulated as CD71^{high} cells as contrasted with wild-type controls which advanced as CD71[med] Ter119^{pos} progenitors (Fig. 7*D*). Third, when Ter119^{pos} progenitors were analyzed by forward-angle light scatter (FALS), a high-FALS subset that was clearly represented in wild-type controls was markedly under-represented among pA2gata1-DYRK3 erythroblasts (Fig. 7*E*). Overall, these obser-

vations for transgenic pA2gata1-DYRK3 mice and pro-erythroblasts consistently indicate inhibitory roles for DYRK3 during late erythropoiesis.

NFAT as a Candidate DYRK3 Target within Erythroid Progenitor Cells—While the present investigations were in progress, Gwack *et al.* (38) discovered via a *Drosophila* transcriptome-wide small interfering RNA approach, that DYRK kinases can regulate NFAT signaling. This was further demonstrated to involve DYRK phosphorylation of NFAT at a key SP-3 motif. To functionally test whether DYRK3 might exert similar effects within erythroid progenitor cells, the following approach was used. First, a K562 cell line model encoding a single-copy-integrated NFAT-specific transcriptional reporter was obtained, and conditions were optimized for specific A23187 ionophore plus phorbol 12-myristate 13-acetate induction of luciferase readouts. This line (designated K562-NFAT-Luc) was then stably transduced with a MIEG3 retroviral vector encoding DYRK3 (or with an empty MIEG3 control vector *per se*). Transduced GFP^{pos} cells then were isolated by FACS and assessed for possible affects of DYRK3 on NFAT-dependent transcription. DYRK3 proved to efficiently inhibit NFAT (Fig. 8*A*). This was observed reproducibly in repeated experiments and in independently transduced and FACS-isolated K562-NFAT-Luc populations (ectopic expression of DYRK3 also was confirmed by Western blotting; data not shown).

Related experiments aimed to assess possible associations between DYRK3 and NFAT in primary bone marrow-derived erythroid cells. We first sought to discover which of five NFAT family members was predominantly expressed in primary erythroid progenitor cells. Reverse transcription-PCR analyses showed NFATc3 to predominate in both early and later stage erythroblasts (Fig. 8*B*). Three commercially available antibodies to DYRK3 were tested next for utility in Western blotting or immunoprecipitations. Unfortunately, none proved to react specifically with DYRK3. One DYRK3 peptide which was used within our laboratory to immunize rabbits, however, yielded antiserum which efficiently and specifically immunoprecipitated (but did not Western blot) DYRK3. The utility of this antiserum for immunoprecipitation is illustrated in Fig. 8*C, left panel*. Finally, antiserum #69 to this peptide was used to immunoprecipitate DYRK3 from *ex vivo* primary erythroblasts as expanded from $DYRK3^{+/+}$ bone marrow and from $DYRK3^{-/-}$ bone marrow as a negative control. Immunoprecipitates were then assayed via Western blotting for possible co-immunoprecipitation of NFATc3 (Fig. 8*D*). NFATc3 proved to co-immunoprecipitate with DYRK3. This finding further suggests that one action of DYRK3 in erythroid progenitor cells involves the modulation of NFAT signaling.

DISCUSSION

As outlined above, DYRK dual-specificity kinases have evolved in yeast, mold, flies, mouse, and man to exert important effects on cell growth and development. In *S. cerevisiae* and in *Dictyostelium*, YAK1p and YAK-A function as nutrient stress transducers and inhibit growth via the modulation of upstream developmental regulators (*e.g.* Pop2p and CprD (16, 17)). In human cell lines, a perhaps analogous role recently has been

(A1)

(A2)

(B)

(C)

(D)

(E)
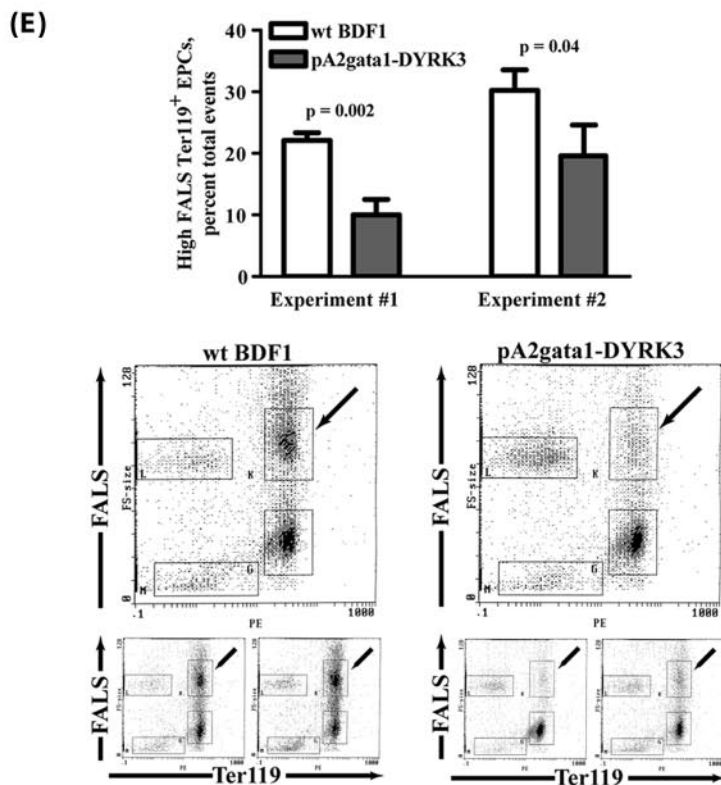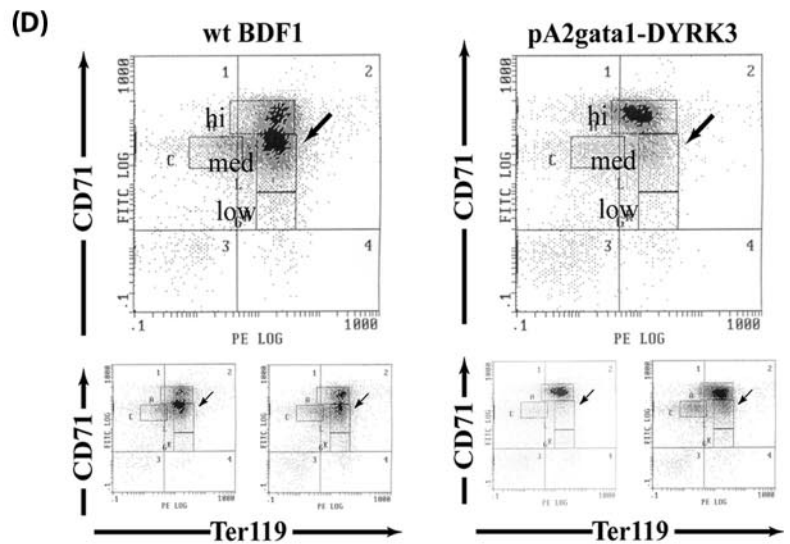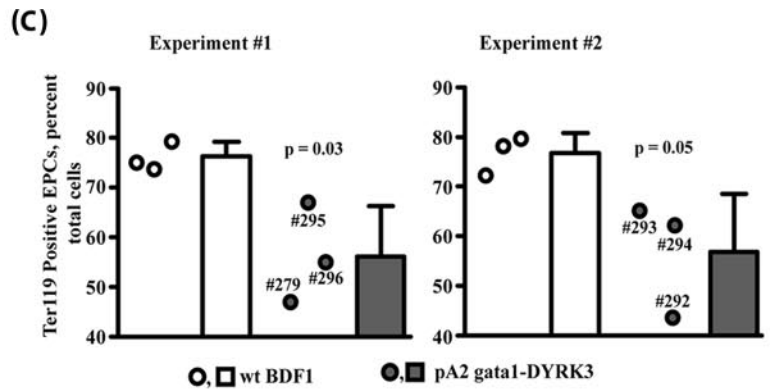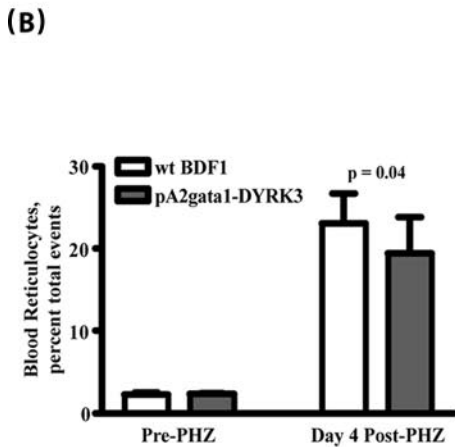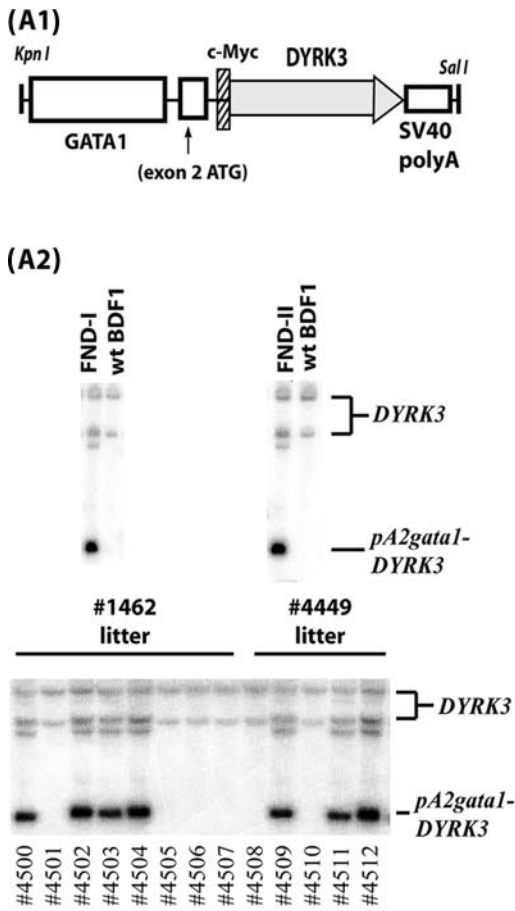
outlined for DYRK2. Specifically, DYRK2 has been demonstrated to act in a stress-sensing mode and to phosphorylate p53 at Ser-46 in response to genotoxic events (32). This action of DYRK2 then reinforces negative effects of p53 on cell growth and survival. By comparison and among DYRK kinases, DYRK3 is most related to DYRK2 in its genomic and protein structure (33). We now suggest that DYRK3 may act in a similar functional modality as an overall suppressor of cell growth but in a selective fashion due to its erythroid lineage-restricted expression profile (14, 15) and its selective action during stress but not steady-state erythropoiesis (see Figs. 2–6). Furthermore (and again like DYRK2; see below), DYRK3 may exert its effects in part by modulating NFAT signaling as one candidate target pathway within erythroid progenitor cells. Findings in support of this hypothesis are outlined below and are discussed further in the contexts of which erythroid progenitor pools might be regulated by DYRK3, what effectors DYRK3 might modulate, how DYRK3 itself might be regulated, and how DYRK3 key actions might be limited to a stress erythropoietic modality.

With regard to the overall effects of DYRK3 on stress erythropoiesis, four present sets of observations point toward an early colony forming unit-erythroid-like compartment as a target for DYRK3 suppression. First, in DYRK3-null mice, advantaged effects on the erythron during anemia were more significant when early progenitors were taxed by 5-fluorouracil dosing or marrow transplantation. Phenylhydrazine-induced hemolysis of mature red cells by comparison led to elevated reticulocyte production in the absence of DYRK3 but did not result in obvious advantages in red cell mass. Second, at steady state, levels of BFUe in the spleens of DYRK3-null mice were somewhat elevated over $DYRK3^{+/+}$ congenic controls. Third, *ex vivo* analyses of primary bone marrow erythroid progenitors revealed apparent increases in the proliferative capacity of $DYRK3^{-/-}$ (pro)erythroblasts as based both on rates of EPO-dependent [3]HdT incorporation and on the cumulative formation of Ter119^{pos} erythroblasts. Fourth, transgenic expression of

DYRK3 in pA2gata1-DYRK3 mice attenuated reticulocyte production during anemia as well as the formation of late-stage (pro)erythroblasts *ex vivo* (see Fig. 7, *A–E*). Overall, the above findings suggest that DYRK3 normally might dampen the average frequency of cell cycling among early stage erythroblasts. Cell cycle entry is a dynamic feature of erythroid progenitors, especially during stress erythropoiesis (5, 45) and, therefore, is a rational component to consider for intrinsic erythroblast negative regulation.

As supported by the present studies, the hypothesis that DYRK3 may exert its prime effects selectively during stress erythropoiesis also raises basic questions concerning the regulation of DYRK3 *per se*. Analyses of *DYRK3* transcript levels in developing erythroblasts indicated not only persistent but apparently increased expression at late stages.[3] The present lack of DYRK3 antibodies which are useful for Western blotting, however, limits the ability to test possible effects of anemia on DYRK3 levels and/or catalytic activity. Interestingly, and for at least DYRK1a and DYRK2, phosphorylation at a unique YXY activation loop recently has been indicated to occur intramolecularly during translation (46). A subsequent apparent burying of this phosphorylated YXY loop is then thought to act to constitutively stimulate DYRKs as S/T-directed kinases (46). This predicts that regulation might occur primarily via lineage-restricted expression mechanisms but does not discount possible regulation via subcellular localization, S/T phosphorylation, and/or partnered effectors. Such candidate mechanisms are under active investigation. Analyses to date, however, do not support the notion that EPO or anemia *per se* affect DYRK3 catalytic activity (negative results, unpublished results[3]). A prospect also exists that substrates for DYRK3 might be lim-

---

[3] O. Bogacheva, O. Bogachev, M. Menon, A. Dev, E. Houde, E. I. Valoret, H. M. Prosser, C. L. Creasy, S. J. Pickering, E. Grau, K. Rance, G. P. Livi, V. Karur, C. L. Erickson-Miller, and D. M. Wojchowski, unpublished result.

FIGURE 7. **pA2*gata1* transgene-mediated expression of DYRK3 inhibits proerythroblast development.** *A*, transgenic pA2gata1-DYRK3 mice construction. *Panel A1*, shown diagrammatically is the construct used to prepare pA2gata1-Myc-DYRK3 mice. *Panel A2*, pA2gata1-Myc DYRK3 founders FND-I and FND-II as analyzed via Southern blotting. Also illustrated (for FND-II) is transgene germ line transmission (*lower sub-panel*) (mice are identified by number, which correspond to those used in the following experiments). *B*, phenylhydrazine (*PHZ*)-induced reticulocyte production is attenuated in pA2gata1-DYRK3 mice. Phenylhydrazine (60 mg/kg) was administered at 1 and 24 h. Note the decrease in reticulocyte production among $Dyrk3^{-/-}$ mice ($n = 5$, mean ± S.D.). In this model hematocrits were not substantially affected (potentially due to compensatory events and/or stage-specific transgene effects). *wt*, wild type. *C*, frequencies of Ter119^{pos} splenic pro-erythroblasts are decreased in pA2gata1-DYRK3 mice. At day 5 post-phenylhydrazine dosing, splenocytes were assayed for Ter119 positivity by flow cytometry. Scatter points represent individual mice. *Bar graphs* represent means and S.D. within each group (*i.e.* wild-type controls *versus* pA2gata1-Dyrk3 mice). Ter119-positive cell frequencies are expressed as a percentage of total splenocytes. *Left panel*, in experiment #1, wild type B6D2F1 splenocytes were 76.7 ± 4.1% Ter119^{pos}, whereas pA2gata1-DYRK3 splenocytes were 56.9 ± 11.7% Ter119^{pos} ($p = 0.03$). *Right panel*, in experiment #2, Ter119^{pos} cell frequencies were 76.3 ± 2.9% for wild-type splenocytes *versus* 56.2 ± 10.2% for pA2gata1-DYRK3 splenocytes ($p = 0.05$). In each independent experiment, values for Ter119^{pos} cell frequencies of pA2gata1-DYRK3 splenocytes were less than 75% that of wild-type control values. *EPC*, erythroid progenitor cells. *D*, Ter119^{pos} erythroid progenitor cells from pA2gata1-DYRK3 mice accumulate as a CD71^{high} subpopulation. To examine the staged-ness of Ter119^{pos} progenitors in splenocytes from phenylhydrazine-treated DYRK3 mice, Ter119 and CD71 expression levels were co-analyzed by flow cytometry; plotted are CD71 positivity *versus* Ter119 positivity for wt B6D2F1 (*left*) and pA2gata1-DYRK3 (*right*) splenocyte preparations. The gated populations are Ter119^{pos} cells expressing CD71 at high, medium, and low levels. These levels of CD71 expression previously have been shown to correlate with size and staged-ness such that earlier, larger (pro) erythroblasts express higher levels of CD71. Note the markedly attenuated development from CD71^{high} to CD71[med] stages among pA2gata1-DYRK3 cells. *Lower panels* illustrate primary data from duplicate analyses. *E*, erythroid progenitors from spleens of phenylhydrazine-treated pA2gata1-DYRK3 mice form aberrantly as CD71^{high}, but FALS^{low} (pro)erythroblasts. Wild-type and pA2gata1- DYRK3 mice were treated with phenylhydrazine. Erythroid splenocytes were then isolated and cultured for 18 h. Among developing (pro)erythroblasts, distributions of high *versus* low Ter119^{pos} cells were analyzed. *Upper panel*, for two independent experiments, data defining the percentage of FALS[high] Ter119^{pos} proerythroblasts are graphed. For experiment #1, values are 22.1 ± 1.3% for wild-type B6D2F1 mice and 10.1 ± 2.5% for pA2gata1-DYRK3 mice ($p = 0.002$). For experiment #2, data are 30.2 ± 3.3% of wild-type B6D2F1 splenocytes and 19.6 ± 5.0% of pA2gata1-DYRK3 splenocytes are high FALS Ter119^{pos} cells ($p = 0.04$). *Lower panel*, shown are primary flow cytometric data for FALS values *versus* Ter119 expression. The high FALS population (as indicated on each flow diagram with an *arrow*) represents a larger erythroid progenitor cell that is significantly less represented in pA2gata1-DYRK3 mice (*right*) *versus* wt B6D2F1 controls (*left*). Primary data shown are representative of two fully independent experiments.
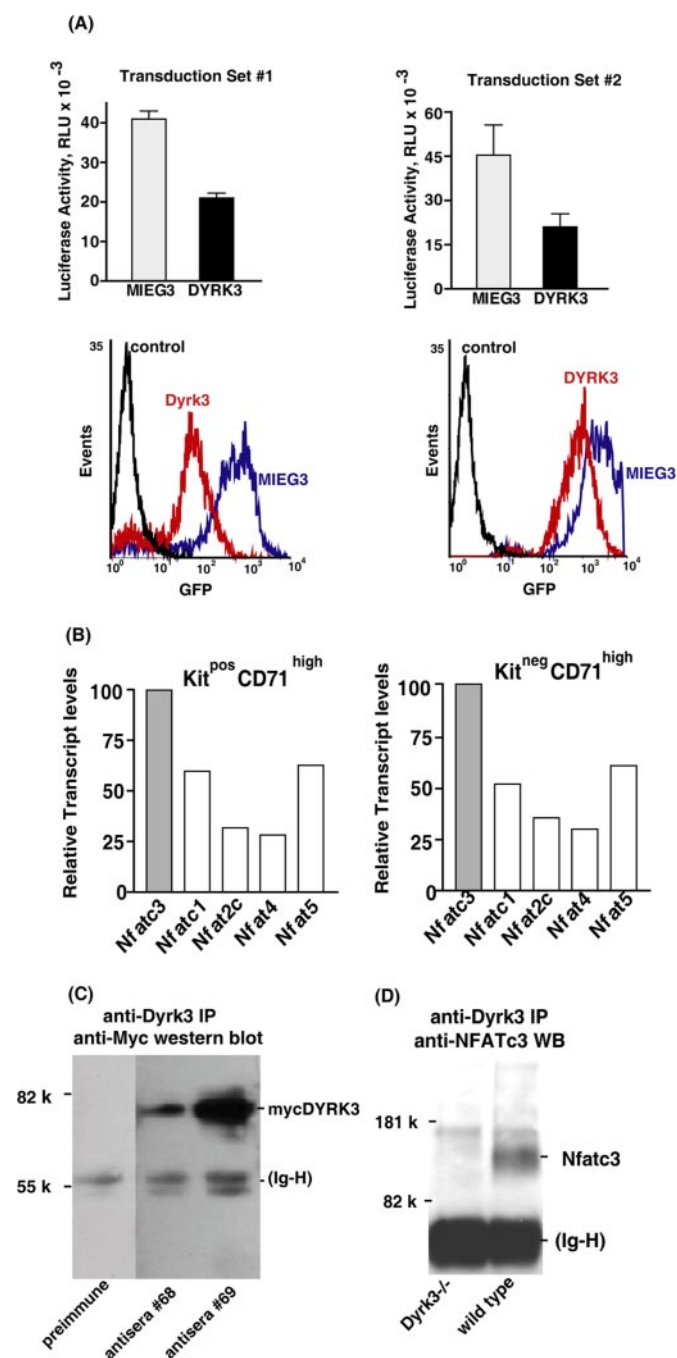
FIGURE 8. **DYRK3 represses NFAT activity in human erythroid K562 cells.**
A, K562-NFAT-Luc cells harboring a stably integrated single copy NFAT-luciferase reporter construct were transduced with a VSV-G packaged MIEG3 retrovirus encoding (Myc)DYRK3 (or in parallel with an empty MIEG3 vector). Stably transduced lines from two independent experiments (*Set 1*, *Set 2*) then were isolated by FACS. Effects of DYRK3 on A23187 plus phorbol 12-myristate 13-acetate-induced NFAT activity then were assessed at 4 h of induction based on NFAT luciferase reporter bioluminescence. *RLU*, relative luciferase units. Graphed values are the means ± S.E. ($n = 4$) and are representative of four independent analyses. *Lower panels* illustrate flow cytometry analyses of transduced and FACS-isolated K562-NFAT-Luc lines. *B*, NFATc3 is the predominant NFAT within primary murine bone marrow-derived erythroblasts. For marrow cell preparations from wild-type C57BL/6 mice, (pro)erythroblasts were expanded in SP34-EX medium. At day 3.5, erythroblasts at Kit^{pos}CD71^{high}Ter119^{neg} and Kit^{neg}CD71^{high}Ter119^{neg} stages were isolated. RNA and cDNA then were prepared, and levels of transcripts were assayed by quantitative PCR for five NFAT orthologues (as indicated). At each stage, note the predominant representation of NFATc3. *C* and *D*, NFATc3 co-immunoprecipitates with endogenous DYRK3 in primary bone marrow-derived erythro-

iting and may themselves be up-modulated during stress erythropoiesis.

Finally, the specific nature of DYRK3 targets (or candidate substrates) also merits discussion. Within their kinase domains, mammalian DYRKs 1a, 1b, 2, 3, and 4 share defining structural motifs. DYRKs 1a and 1b, however, are less related to DYRKs 2–4, possess conserved nuclear localization signals, and unlike DYRKs 2–4, are predominantly nuclear (14–33). DYRKs overall have been argued to act as arginine-directed S/T kinases (21). DYRK1a, in particular, has also been demonstrated to phosphorylate a variety of candidate substrates including the Forkhead transcription factor FKHR (47), cyclin L2 (48), the cytoskeletal and endocytic factor, dynamin (49), elongation factor eIF2Bε (50), and a microtubule-associated Tau protein which can affect neurofibrillary tangles (26, 50). For Tau, DYRK1a also has been suggested to act as a glycogen synthase kinase-3 priming kinase (50). Interestingly, this glycogen synthase kinase 3 priming activity has been argued to be exerted by DYRK2 as studied as a follow-up to the recent discovery of NFATs as DYRK kinase targets in a *Drosophila* S2 cell system (38). In particular, DYRK1a and -2 appear to phosphorylate NFAT within an SP-3 subdomain before phosphorylation by glycogen synthase kinase-3 at an adjacent SP-2 motif (38). As demonstrated using an interleukin-2 promoter-reporter system, overall effects on NFAT were inhibitory. This latter work (as reported during the present studies) prompted our investigation of possible effects of DYRK3 on NFAT activity. In an erythroid cell model, DYRK3 in fact proved to efficiently inhibit NFAT transcriptional capacity. In addition, NFAT3 (SP-3 domain encoding NFAT) was shown to be the predominant NFAT in primary erythroid cells and to co-immunoprecipitate with endogenous DYRK3. Initial efforts to map DYRK3 subdomains that mediate NFAT interactions, however, have not been revealing to date. This may be due to more than static or simple interaction mechanisms. For NFATs, gene disruption experiments indicate redundancy, and functional phenotypes have been best revealed for select tissues via compound knock-out strategies (51, 52). The extent to which such NFAT knockouts might be altered in their erythropoietic capacities remains to be investigated, as does the possibly extended set of DYRK3 targets in (pro)erythroblasts. Overall, the present work indicates that via these routes (and prospective additional targets) DYRK3 plays a meaningful and non-redundant role as an erythropoietic suppressor selectively during stress erythropoiesis. DYRK3, therefore, also comprises an interesting candidate for targeting by small molecule inhibitors as potentially important anti-anemia agents.

blasts. *Panel C* illustrates the utility of a DYRK3 peptide antiserum (#69) to efficiently immunoprecipitate (*IP*) (Myc)DYRK3 as expressed transiently in 293 cells from a pEFNeo vector. In *panel D* erythroid progenitor cells were expanded in (SP34-EX medium) from bone marrow preparations from *DYRK3*$^{-/-}$ and wild-type *DYRK3*$^{+/+}$ mice. Erythroblasts then were isolated, washed, and lysed. Lysates were subjected to immunoprecipitation using DYRK3 peptide antiserum #69. Immunoprecipitates were then assayed for the co-immunoprecipitation of NFATc3 via Western blotting (*WB*).

REFERENCES

1. Munugalavadla, V., and Kapur, R. (2005) *Crit. Rev. Oncol. Hematol.* **54,** 63–75
2. Lenox, L. E., Perry, J. M., and Paulson, R. F. (2005) *Blood* **105,** 2741–2748
3. Menon, M. P., Karur, V., Bogacheva, O., Bogachev, O., Cuetara, B., and Wojchowski, D. M. (2006) *J. Clin. Investig.* **116,** 683–694
4. Bauer, A., Tronche, F., Wessely, O., Kellendonk, C., Reichardt, H. M., Steinlein, P., Schutz, G., and Beug, H. (1999) *Genes Dev.* **13,** 2996–3002
5. Longmore, G. D. (2006) *J. Clin. Investig.* **116,** 626–628
6. Socolovsky, M., Murrell, M., Liu, Y., Pop, R., Porpiglia, E., and Levchenko, A. (2007) *PLoS Biol.* **5,** e252
7. Mirandola, P., Gobbi, G., Ponti, C., Sponzilli, I., Cocco, L., and Vitale, M. (2006) *Blood* **107,** 508–513
8. Lyons, B. L., Lynes, M. A., Burzenski, L., Joliat, M. J., Hadjout, N., and Shultz, L. D. (2003) *Exp. Hematol.* **31,** 234–243
9. Callero, M. A., Perez, G. M., Vittori, D. C., Pregi, N., and Nesse, A. B. (2007) *Cell. Physiol. Biochem.* **20,** 319–328
10. Sarna, M. K., Ingley, E., Busfield, S. J., Cull, V. S., Lepere, W., McCarthy, D. J., Wright, M. J., Palmer, G. A., Chappell, D., Sayer, M. S., Alexander, W. S., Hilton, D. J., Starr, R., Watowich, S. S., Bittorf, T., Klinken, S. P., and Tilbrook, P. A. (2003) *Oncogene* **22,** 3221–3230
11. Nonami, A., Kato, R., Taniguchi, K., Yoshiga, D., Taketomi, T., Fukuyama, S., Harada, M., Sasaki, A., and Yoshimura, A. (2004) *J. Biol. Chem.* **279,** 52543–52551
12. Tong, W., Zhang, J., and Lodish, H. F. (2005) *Blood* **105,** 4604–4612
13. Li, Z., Zhou, Y., Carter-Su, C., Myers, M. G., Jr., and Rui, L. (2007) *Mol. Endocrinol.* **21,** 2270–2281
14. Lord, K. A., Creasy, C. L., King, A. G., King, C., Burns, B. M., Lee, J. C., and Dillon, S. B. (2000) *Blood* **95,** 2838–2846
15. Geiger, J. N., Knudsen, G. T., Panek, L., Pandit, A. K., Yoder, M. D., Lord, K. A., Creasy, C. L., Burns, B. M., Gaines, P., Dillon, S. B., and Wojchowski, D. M. (2001) *Blood* **97,** 901–910
16. Moriya, H., Shimizu-Yoshida, Y., Omori, A., Iwashita, S., Katoh, M., and Sakai, A. (2001) *Genes Dev.* **15,** 1217–1228
17. Taminato, A., Bagattini, R., Gorjao, R., Chen, G., Kuspa, A., and Souza, G. M. (2002) *Mol. Biol. Cell* **13,** 2266–2275
18. Stitzel, M. L., Pellettieri, J., and Seydoux, G. (2006) *Curr. Biol.* **16,** 56–62
19. Tejedor, F., Zhu, X. R., Kaltenbach, E., Ackermann, A., Baumann, A., Canal, I., Heisenberg, M., Fischbach, K. F., and Pongs, O. (1995) *Neuron* **14,** 287–301
20. Becker, W., and Joost, H. G. (1999) *Prog. Nucleic Acid Res. Mol. Biol.* **62,** 1–17
21. Campbell, L. E., and Proud, C. G. (2002) *FEBS Lett.* **510,** 31–36
22. Epstein, C. J. (2006) *Nature* **441,** 582–583
23. Fotaki, V., Dierssen, M., Alcantara, S., Martinez, S., Marti, E., Casas, C., Visa, J., Soriano, E., Estivill, X., and Arbones, M. L. (2002) *Mol. Cell. Biol.* **22,** 6636–6647
24. Benavides-Piccione, R., Dierssen, M., Ballesteros-Yanez, I., Martinez de Lagran, M., Arbones, M. L., Fotaki, V., DeFelipe, J., and Elston, G. N. (2005) *Neurobiol. Dis.* **20,** 115–122
25. Ahn, K. J., Jeong, H. K., Choi, H. S., Ryoo, S. R., Kim, Y. J., Goo, J. S., Choi, S. Y., Han, J. S., Ha, I., and Song, W. J. (2006) *Neurobiol. Dis.* **22,** 463–472
26. Kim, E. J., Sung, J. Y., Lee, H. J., Rhim, H., Hasegawa, M., Iwatsubo, T., Min do, S., Kim, J., Paik, S. R., and Chung, K. C. (2006) *J. Biol. Chem.* **281,** 33250–33257
27. Adayev, T., Chen-Hwang, M. C., Murakami, N., Wang, R., and Hwang, Y. W. (2006) *Biochem. Biophys. Res. Commun.* **351,** 1060–1065
28. Mercer, S. E., Ewton, D. Z., Shah, S., Naqvi, A., and Friedman, E. (2006) *Cancer Res.* **66,** 5143–5150
29. Deng, X., Ewton, D. Z., Li, S., Naqvi, A., Mercer, S. E., Landas, S., and Friedman, E. (2006) *Cancer Res.* **66,** 4149–4158
30. Jin, K., Park, S., Ewton, D. Z., and Friedman, E. (2007) *Cancer Res.* **67,** 7247–7255
31. Sacher, F., Moller, C., Bone, W., Gottwald, U., and Fritsch, M. (2007) *Mol. Cell. Endocrinol.* **267,** 80–88
32. Taira, N., Nihira, K., Yamaguchi, T., Miki, Y., and Yoshida, K. (2007) *Mol. Cell* **25,** 725–738
33. Zhang, D., Li, K., Erickson-Miller, C. L., Weiss, M., and Wojchowski, D. M. (2005) *Genomics* **85,** 117–130
34. Pratt, Z. L., Drehman, B. J., Miller, M. E., and Johnston, S. D. (2007) *J. Mol. Biol.* **368,** 30–43
35. Li, K., Zhao, S., Karur, V., and Wojchowski, D. M. (2002) *J. Biol. Chem.* **277,** 47052–47060
36. Miller, C. P., Heilman, D. W., and Wojchowski, D. M. (2002) *Blood* **99,** 898–904
37. Zhang, D., Johnson, M. M., Miller, C. P., Pircher, T. J., Geiger, J. N., and Wojchowski, D. M. (2001) *Exp. Hematol.* **29,** 1278–1288
38. Gwack, Y., Sharma, S., Nardone, J., Tanasa, B., Iuga, A., Srikanth, S., Okamura, H., Bolton, D., Feske, S., Hogan, P. G., and Rao, A. (2006) *Nature* **441,** 646–650
39. Sytkowski, A. J. (2007) *Sci. STKE 2007,* pe38
40. Menon, M. P., Fang, J., and Wojchowski, D. M. (2005) *Blood* **107,** 2662–2672
41. Pircher, T. J., Zhao, S., Geiger, J. N., Joneja, B., and Wojchowski, D. M. (2000) *Oncogene* **19,** 3684–3692
42. Socolovsky, M., Nam, H., Fleming, M. D., Haase, V. H., Brugnara, C., and Lodish, H. F. (2001) *Blood* **98,** 3261–3273
43. Kina, T., Ikuta, K., Takayama, E., Wada, K., Majumdar, A. S., Weissman, I. L., and Katsura, Y. (2000) *Br. J. Haematol.* **109,** 280–287
44. Quinn, J., Fisher, P. W., Capocasale, R. J., Achuthanandam, R., Kam, M., Bugelski, P. J., and Hrebien, L. (2007) *Cytometry A* **71,** 612–624
45. Fang, J., Menon, M., Kapelle, W., Bogacheva, O., Bogachev, O., Houde, E., Browne, S., Sathyanarayana, P., and Wojchowski, D. M. (2007) *Blood* **110,** 2361–2370
46. Lochhead, P. A., Sibbet, G., Morrice, N., and Cleghon, V. (2005) *Cell* **121,** 925–936
47. Woods, Y. L., Rena, G., Morrice, N., Barthel, A., Becker, W., Guo, S., Unterman, T. G., and Cohen, P. (2001) *Biochem. J.* **355,** 597–607
48. de Graaf, K., Hekerman, P., Spelten, O., Herrmann, A., Packman, L. C., Bussow, K., Muller-Newen, G., and Becker, W. (2004) *J. Biol. Chem.* **279,** 4612–4624
49. Chen-Hwang, M. C., Chen, H. R., Elzinga, M., and Hwang, Y. W. (2002) *J. Biol. Chem.* **277,** 17597–17604
50. Woods, Y. L., Cohen, P., Becker, W., Jakes, R., Goedert, M., Wang, X., and Proud, C. G. (2001) *Biochem. J.* **355,** 609–615
51. Winslow, M. M., Pan, M., Starbuck, M., Gallo, E. M., Deng, L., Karsenty, G., and Crabtree, G. R. (2006) *Dev. Cell* **10,** 771–782
52. Ranger, A. M., Oukka, M., Rengarajan, J., and Glimcher, L. H. (1998) *Immunity* **9,** 627–635